Physica E 64 (2014) 106–111

Contents lists available at ScienceDirect

Physica E

journal homepage: www.elsevier.com/locate/physe

Structural characterizations and optical properties of InSe and InSe:Ag semiconductors grown by Bridgman/Stockbarger technique

Bekir Gürbulak [a], Mehmet Şata [a], Seydi Dogan [b], Songul Duman [a,*], Afsoun Ashkhasi [a], E. Fahri Keskenler [c]

[a] Department of Physics, Faculty of Sciences, Atatürk University, 25240 Erzurum, Turkey
[b] Department of Electrical and Electronics Engineering, Faculty of Engineering and Architecture, Balikesir University, Balikesir 10145, Turkey
[c] Department of Nanotechnology Engineering, Faculty of Engineering, Recep Tayyip Erdoğan University, Rize 53100, Turkey

HIGHLIGHTS

- The effects of Ag doping on structural and optical properties of InSe crystal.
- Increase in the intensity of all diffraction peaks and disappearance of impurities with Ag doping.
- Increase in the energy band gap and the first exciton energy values.

ARTICLE INFO

Article history:
Received 25 April 2014
Received in revised form
20 June 2014
Accepted 2 July 2014
Available online 16 July 2014

Keywords:
InSe
InSe:Ag
Single crystals
First exciton energy
Structural analysis

ABSTRACT

Undoped InSe and Ag doped InSe (InSe:Ag) single crystals have been grown by using the Bridgman/Stockbarger method. The freshly cleaved crystals have mirror-like surfaces even without using mechanical treatment. The structure and lattice parameters of the undoped InSe and InSe:Ag semiconductors have been analyzed using a X-ray diffractometer (XRD), Scanning electron microscopy (SEM) and energy dispersive X-rays (EDX) techniques. It is found that the InSe and InSe:Ag crystals had hexagonal structure, and calculated lattice constants were found to be $a=4.002$ Å and $c=17.160$ Å for InSe and $a=4.619$ Å and $c=17.003$ Å for InSe:Ag. The crystallite sizes have been calculated to be 40–150 nm for InSe and 75–120 nm for InSe:Ag from the SEM results. Ag doping causes a significant increase in the XRD peak intensity. It has been observed from EDX results that InSe contains In=57.12%, Se=38.08% and O=4.81%, respectively. Absorption measurements have been carried out in InSe and InSe:Ag samples in the temperature range 10–320 K with a step of 10 K. The first exciton energies for $n=1$ were calculated as 1.328, 1.260 eV in InSe and were 1.340, 1.282 eV in InSe:Ag at 10 K and 320 K, respectively.

© 2014 Elsevier B.V. All rights reserved.

1. Introduction

It is well known that the single crystals of $A^{III}B^{VI}$ type compounds, in particular of Indium Selenide (InSe), crystallize in a layered structure where each layer contains two In and two Se close-packed sub layers with the stacking sequence Se–In–In–Se [1]. InSe is a layered semiconductor, which can be cleaved to yield high-quality surfaces and has been shown a new class of materials for solar energy conversion applications [2–4]. The bonding between two adjacent layers is of the weak Van der Waals type, while within the layer the bonding is predominantly covalent. Depending on the packing of the layers the indicated single crystals form various modifications, in which the positions of band edges are determined by interlayer interactions. Binary semiconductor compounds such as InSe are of widespread technological and scientific interest owing to their practical applications in the areas of visible and infrared light emitting diodes, infrared detectors, optical parametric oscillators, nonlinear optics, solar cells, optical frequency conversion, second harmonic generation devices and many other electro-optical devices.

Although semiconducting compound thin films on conducting substrates have attracted much attention in recent years for the fabrication of solar cells and there are a number of deposition techniques such as vacuum evaporation [5], molecular beam epitaxy [6], flash evaporation [7], chemical vapour deposition [8], Van der Walls epitaxy [9]. The Bridgman/Stockbarger technique is an inexpensive, needing no substrate, simple and low temperature growth method that could produce high quality bulk semiconductors for the

* Corresponding author. Tel.: +90 442 231 4075 (work).
E-mail address: sduman@atauni.edu.tr (S. Duman).

http://dx.doi.org/10.1016/j.physe.2014.07.002
1386-9477/© 2014 Elsevier B.V. All rights reserved.

device applications such as heterojunction devices with a very low interface density of states, switching devices etc.

Balitskii et al. have used the methods of cathodoluminescence analysis and of X-ray diffraction (XRD) to study the chemical phase compositions of InSe films [10]. Structural studies showed the presence of In_4Se_3 with InSe [11]. XRD spectrum has revealed that the synthesized products are single-crystalline of the β-phase hexagonal structure of InSe with lattice parameters $a=4.006$ Å and $c=16.642$ Å. The strong peak due to the reflection from the (0 0 4) crystal plane reveals that most nanowires grow with a strong preferred orientation [12]. The crystal structure of the ϒ-In_2Se_3 films were determined by X-ray diffraction and Raman spectroscopy in a study carried out by Ref. [13]. From the temperature dependence of the free exciton line, the room-temperature energy gap of ϒ-In_2Se_3 film was found to be about 1.947 eV [13]. Highly oriented InSe films had been prepared onto heated quartz substrates using the co-evaporation technique with 20% Se over pressure followed by 1 h annealing at the growth temperature and were characterized by XRD, Raman spectroscopy and atomic force microscopy [14]. A comprehensive study on the synthesis, characterization, and thin film photodetector application of atomic layers of InSe has been carried out by Sidong et al. [15].

In literature, measurements of absorbance and transmittance in In_xSe_{1-x} thin films in the spectral range of 1.1 to 3.9 eV carried out at room temperature [16]. Gürbulak et al. have grown InSe:Ho single crystals by a method which is similar to the direct freezing. The first exciton energy values for $n=1$ were calculated as 1.315 eV in n-InSe: Ho, 1.331 eV in InSe and 1.326 eV in InSe:Dy at 10 K [17]. Ateş et al. [18] reported that the absorption edge has shifted towards longer wavelengths and a decrease of intensity in absorption spectra has occured under an electric field of 5 kV/cm. At 10 and 320 K, in InSe the first exciton energies were calculated as 1.350 and 1.311 eV for zero voltage and 1.334 eV 1.301 eV for electric field, respectively. The study carried out by Mudd et al. [19], have shown that the energy position and linewidth of the excitonic recombination in a crystal grown by Bridgman technique could be reproduced for the thin flakes of InSe from about 1 to 10^3 μm^2 in size. In a detailed photoconductivity study carried out by Sidong et al. [15], has been observed that few-layered InSe has an indirect band gap of 1.4 eV, which is 200 meV higher than bulk one and a strong photoresponse of 34.7 mA/W and fast response time of 488 μs for a few layered InSe has been measured.

In this study, undoped InSe and silver (Ag) doped (InSe:Ag) single crystals belonging to the family of III–VI compound semiconductors and used for many technological applications have been grown and their structural and morphological analyses have been carried out at room temperature as well as optical absorption measurement taken between 10 and 320 K. The crystals were prepared by Bridgman/Stockbarger method, starting from synthesized material with a stoichiometric content of In, Se and Ag of purity 5 N. We present the results of the systematic studies on the optical, morphological and structural properties of the InSe and InSe:Ag. The structural and morphological characterization of the crystals were analyzed by means of XRD, energy dispersive X-rays (EDX) and scanning electron microscopy (SEM). The optical absorption measurements were recorded using a Perkin Elmer UV/VIS Lambda 4 S Spectrometer which works in the range of 175–1100 nm and has a wavelength accuracy of better than ±0.3 nm at 10 and 320 K. Therefore, $E_{exc.}$ can be calculated with an accuracy of approximately better than 0.6 meV considering the wavelength accuracy of spectrometer.

2. Experimental procedures

For the constituent of polycrystalline $A^{III}B^{VI}$, the first important step in obtaining high quality crystals is the purity of the basic elements which are being involved in the structure. These elements were weighed in a stoichiometric ratio accurate to 0.1 mg. The total mass of the elements was about 40 g. The basic criteria for this choice were; first a sufficient need to justify the cost of one run, second minimal loss of the material in case of breakage.

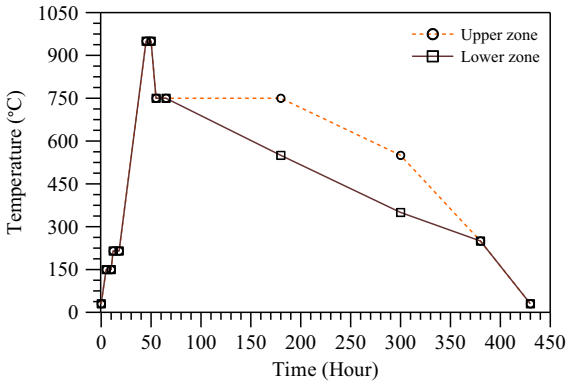

Fig. 1. Growth programme for InSe and InSe:Ag single crystals.

This stoichiometric ratio necessary to produce 40 g InSe was calculated using the following relationships:

$$M_{In} = (M_{Se}/A_{Se})A_{In} \quad (1)$$

with total mass,

$$M_{In} + M_{Se} = 40\ g \quad (2)$$

where, M and A are total and atomic masses, respectively.

InSe and InSe:Ag (0.01 wt% Ag) single crystals were grown by using the Bridgman/Stockbarger method at the same time. The melting point of 660 ± 5 °C [20] of the InSe compound were determined from the phase diagram. Sealed quartz ampoule was annealed at 950 °C for 15 h in the out gassing furnace designed in our laboratories. The temperature of quartz ampoule was decreased to room temperature in 24 h. The mix In–Se (0.01 wt% Ag) put into quartz ampoule and quartz ampoule was sealed under a vacuum of 10^{-6} mbar. Quartz ampoules were coated with carbon. The crucible was suspended in the middle of the vertical furnace with two zone designed. Growth programme of InSe and InSe:Ag single crystals have been given in Fig. 1. The temperature of furnace was increased to 950 °C and stayed at that temperature for 40 h and then decreased to 750 °C and stayed at that temperature for 15 h. The temperature of lower zone of furnace was reduced to 250 °C at a rate of 1.54 °C/h. Both of the furnace zones cooled to 250 °C in 75 h. The solidified ingot was cooled to room temperature in 50 h.

The prepared InSe and InSe:Ag single crystal ingots were 10 mm in diameter and about 60 mm in length. The ingots had no cracks or voids on the surface. No polishing or cleaning treatments were carried out on the cleaved faces of the samples because of the natural mirror-like cleavage faces. They were cleaved into perpendicular planes of naturally cleaved planes. Pure InSe and InSe:Ag samples were cleaved from the ingots with a razor blade and cut into 48 ± 5 μm and 50 ± 5 μm thick and about 3 × 4.2 mm^2 and 4 × 3.3 mm^2 in sizes. It is found that the grown samples have a n-type conductivity using hot-probe technique.

3. Basic equations

From the XRD profiles, the inter-planar spacing d_{hkl} was calculated for the (0 0 4) plane using the Bragg's relation [21].

$$d_{hkl} = \frac{n\lambda}{2\ \mathrm{Sin}\ \theta} \quad (3)$$

where λ is the wavelength of the X-ray used, d is the lattice spacing, n (n=1,2,3,…) is the order number and θ is the Braggs angle. The factor d is related to ($h\,k\,l$) indices of the planes and the dimension of the unit cells. The peak width at half maximum used to determine the crystallite size (D) by using Debye–Scherrer formula is,

$$D=\frac{K\lambda}{(\beta\ \mathrm{Cos}\ \theta)} \tag{4}$$

where K=0.94 is the Scherrer constant, λ=1.54056 Å is the wavelength of the X-ray radiation, β is the full width at half maximum in radians and θ is the Bragg diffraction angle. The strain (ε) value may be evaluated using the relation

$$\varepsilon=\frac{(\beta\ \mathrm{Cos}\ \theta)}{4} \tag{5}$$

The dislocation density (δ) may be calculated by using the formula [22].

$$\delta=\frac{15\varepsilon}{(axD)} \tag{6}$$

The absorption coefficients were obtained from transmission data using relationship

$$T=(1-R)^2\exp(-A)=(1-R)^2\exp(-\alpha d) \tag{7}$$

where R is reflectivity A is absorbance, α is absorption coefficient and d is sample thickness.

The change of the band gap with temperature is given as following:

$$\frac{dE_g}{dT}=\left(\frac{dE_g}{dT}\right)_{l-ex}+\left(\frac{dE_g}{dT}\right)_{e-p}, \tag{8}$$

where the first and second terms depend on crystal lattice thermal expansion and electron–phonon interaction, respectively.

In most semiconductors, the following empirical expression suggested by Varshni is used to describe the temperature dependence of the excitonic transition energy [23]:

$$E_{ex}(T)=E_{ex}(0)-\delta\frac{T^2}{T+\beta} \tag{9}$$

where $E_{ex}(T)$ is the excitonic energy at sample temperature T, $E_{ex}(0)$ is the excitonic transition energy at 0 K, and δ and β are parameters being characteristics of the material. The parameter β is usually used to estimate of Debye temperature (θ_D).

4. Results and discussion

The structural characterization of the single crystals deposited films were analyzed by means of XRD measurements, SEM and EDX. The structural and lattice parameters of the InSe and InSe:Ag semiconductors were analyzed using a X-ray diffractometer (XRD) using Cu-$K\alpha$ radiation with a wavelength of λ=1.54050 Å (Rigaku Miniflex). The values of 2θ were altered between 10° and 90° with the step of 0.1°/s. Fig. 2 shows the XRD pattern of the undoped InSe and InSe:Ag semiconductors. It is found that the InSe and InSe:Ag crystals had hexagonal structure and giving a dominant diffraction peak around 2θ=66,880° being (0 0 1 2) plane. This result is in a good agreement with that obtained by Refs. [24–29]. In addition to this (0 0 1 2) peak, some other peaks corresponding to (0 0 4) [24–26,28,30,31], (0 0 6) [24–26,28,30,31], (0 0 8) [26,28,30], (3 1 1) [24,31], (0 2 7) [28,30–33] and (0 0 1 8) [31], orientations were also observed. The results given in Fig. 2 are in good agreement with those in the literature.

The values of standard interplanar distance (d_0) and observed interplanar distance (D_{exp}) calculated by using Eq. (3) along with their respective planes for InSe and InSe:Ag semiconductors have

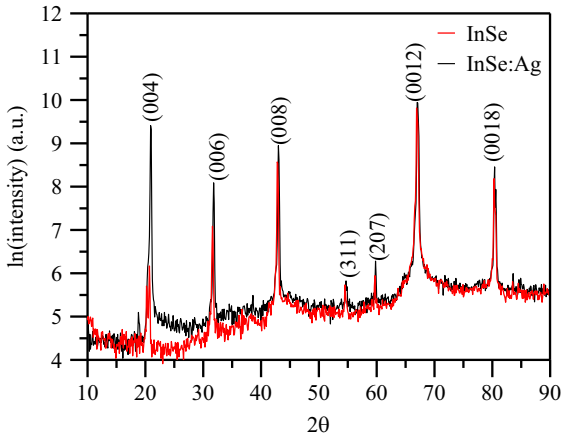

Fig. 2. X-ray diffraction (XRD) spectra of InSe and InSe:Ag after annealing (T=300 °C, 4 h). The Miller indices are indicated on each diffraction peak.

Table 1
The XRD results for the undoped InSe ve InSe:Ag.

Peak	Sample	2θ	Intensity	Int. ratio	d_o	$d_{exp.}$	Structure
(0 0 4)	InSe	20.68	449.07	27.08	4.170	4.290	Hexagonal
	InSe:Ag	20.88	12,161.62		4.170	4.251	
(0 0 6)	InSe	31.62	1,156.57	2.82	2.773	2.827	Hexagonal
	InSe:Ag	31.77	3,255.89		2.918	2.814	
(0 0 8)	InSe	42.85	5,228.96	1.47	2.080	2.109	Hexagonal
	InSe:Ag	43.05	7,670.03		2.103	2.099	
(3 1 1)	InSe	54.51	308.08	1.10	1.663	1.682	Hexagonal
	InSe:Ag	54.70	339.23		1.672	1.676	
(0 2 7)	InSe	59.71	380.47	1.40	1.536	1.547	Hexagonal
	InSe:Ag	59.80	531.99		1.549	1.545	
(0 1 1 2)	InSe	66.88	18,343.43	1.13	1.386	1.398	Hexagonal
	InSe:Ag	66.99	20,776.94		1.394	1.397	
(0 0 1 8)	InSe	80.42	3,555.13	1.32	1.187	1.193	Hexagonal
	InSe:Ag	80.42	4,707.91		1.187	1.193	

been given in Table 1. As clearly seen from Fig. 2 and from intensity ratio data given in Table 1, the XRD peak intensities increase with Ag doping. It causes a significant increase in the XRD peak intensity, and the largest increase in intensity has been observed for the (0 0 4) peak. We believe that the increases in the intensities are mainly due to the disappearance of the impurities which are decreased by Ag doping into the InSe semiconductor. Similar behavior, in the optical properties of InSe, has also been shown with Er doping [34]. The experimental (D_{exp}) interplanar distance values have been calculated by using Bragg diffraction law [35].

The crystallite size, dislocation density and residual strain for the undoped InSe and InSe:Ag have been calculated using the Eqs. (4)-(6), respectively. The analysis results obtained from EDX, SEM and XRD measurements have been presented in Table 2. The lattice parameters a and c of the hexagonal structure of InSe can be calculated using the following relation:

$$\frac{1}{d_{hkl}^2}=\frac{4}{3}\left(\frac{h^2+hk+k^2}{a^2}\right)+\frac{l^2}{c^2} \tag{10}$$

where d is the interplanar distance and ($h\,k\,l$) are the miller indices. The calculated lattice constants were found to be a=4.002 ± 0.004 Å and c=17.160 ± 0.004 Å for InSe and a=4.619 ± 0.004 Å and c=17.003 ± 0.004 Å for InSe:Ag. These values are almost agreed with the ones given in JPCDS card No.: 34-1431 (a=4.005 Å ve c=16.640 Å). The number of crystallites per unit area was

Table 2
The crystallite size (D), dislocation density (ε) and residual strain (δ) for the undoped InSe and InSe:Ag.

Peak	Sample	2θ	D (nm)	ε (lin^{-2}/m^4) $\times 10^{-4}$	δ (lin/m^2) $\times 10^{15}$	N ($\times 10^{17}$ m^{-2}
(0 0 4)	InSe	20.68	58.13	6.29	0.41	2.443
	InSe:Ag	20.88	76.89	4.71	0.20	1.099
(0 0 6)	InSe	31.62	64.27	5.63	0.33	1.808
	InSe:Ag	31.77	78.17	4.63	0.19	1.046
(0 0 8)	InSe	42.85	73.85	4.90	0.25	1.191
	InSe:Ag	43.05	77.95	4.64	0.19	1.055
(0 0 1 2)	InSe	66.88	60.41	5.99	0.37	2.177
	InSe:Ag	66.99	58.77	6.16	0.34	2.463
(0 0 1 8)	InSe	80.42	59.25	6.10	0.39	2.308
	InSe:Ag	80.42	50.97	7.10	0.53	3.776

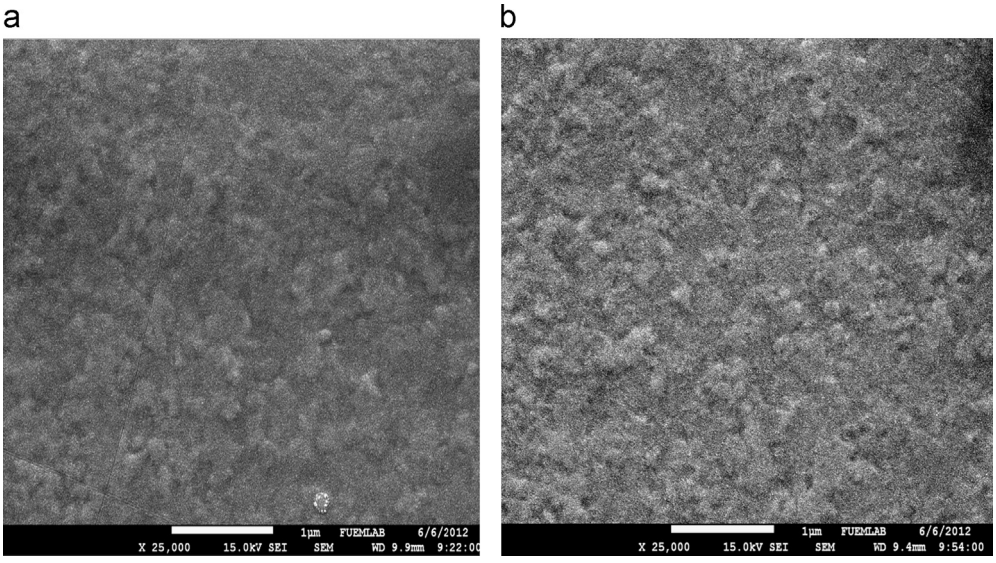

Fig. 3. SEM images taken at 15 kV with a 25,000 magnification for (a) undoped InSe and (b) InSe:Ag crystals.

determined using the relation [36]:

$$N = \frac{d}{D^3} \tag{11}$$

where d is the thickness of the semiconductor crystal.

The surface morphology images of the InSe and InSe:Ag crystals were obtained by (SEM) at 15 kV with a 25,000 magnification. The surfaces of the InSe and InSe:Ag were coated with Au for SEM image enhancement. Fig. 3 shows the SEM images of undoped InSe and InSe:Ag crystals. It can clearly be seen that crystals have smooth and homogeneous surfaces. It has been found that they have a novel hexagonal form and their crystallite sizes being quite close to each other have been calculated to be 40–150 nm for InSe and 75–120 nm for InSe:Ag. These results are in a good agreement with EDX results. Fig. 4 shows the EDX spectra of undoped and InSe and InSe:Ag. The fact that EDX spectrum of InSe crystal is quite close to that of InSe:Ag crystal shows that they have high quality homogeneous surfaces. Similar results have also been observed by Ref. [26]. The doping of Ag element with 0.01% into the InSe has not changed much the structure. In and Se elements have been taken as 61.17%, and 38.83% in order to obtain the stoichiometric ratio being an important issue for the constituent of InSe compound, respectively. However, according to the EDX results, InSe contains In=57.12%, Se=38.08% and O=4.81%, respectively. These values are quite close to the expected ones and a little amount of In has been bonded to O.

The optical absorption measurements have been taken between 10 and 320 K achieved with a closed-cycle helium cryostat using a Perkin Elmer UV/VIS Lambda 4 S Spectrometer. The absorbance data were converted to absorption coefficient values according to the equations described elsewhere in Ref. [37] using Eq. (7). The exciton absorption coefficient of InSe and InSe:Ag samples for different temperatures (10, 160 and 320 K) are shown in Fig. 5. Analysing the experimental data for InSe and InSe:Ag samples, we found that absorption coefficients of InSe are between 144 and 714 cm^{-1} and of InSe:Ag are between 141 and 768 cm^{-1} at 10 K, respectively (see Fig. 5). The exciton absorption edges of both the investigated compounds shifted considerably when the temperature was changed from 10 to 320 K. As seen Fig. 5, the exciton absorption spectra of InSe are smaller than that of InSe:Ag. Ag doping in the InSe changes the exciton absorption spectrum in the high-energy region. Ag doping to InSe caused an increasing in absorption peak intensities. As can be seen in Fig. 6, the absorption edge shifts towards to shorter wavelengths and band gap energy increases by Ag doping. As can be seen Table 3, when doped Ag into the InSe sample, the electrons stimulate from valence band to conductivity band, for this reason the electron concentration decreases in valence band resulting the absorption intensity decrease.

The experimental results for the temperature dependence of the first excitonic structure for undoped and Ag doped samples in the temperature range of 10–320 K are respectively shown in Fig. 6. The first exciton levels were determined. The energy of the first exciton level for InSe and InSe:Ag samples are given in Table 3. It is evident that the first exciton energies decrease with

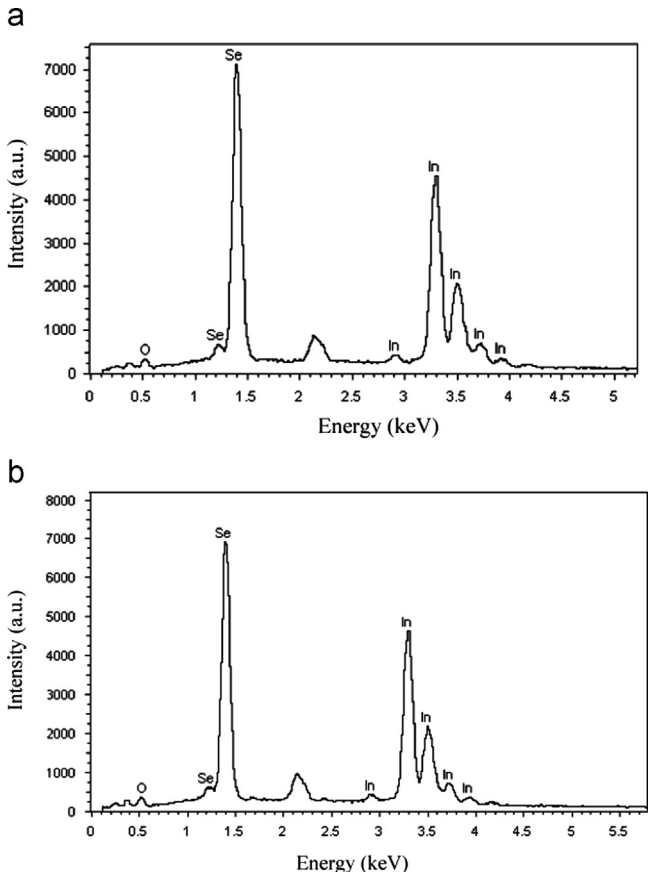

Fig. 4. EDX spectra for (a) InSe and (b) InSe:Ag crystals.

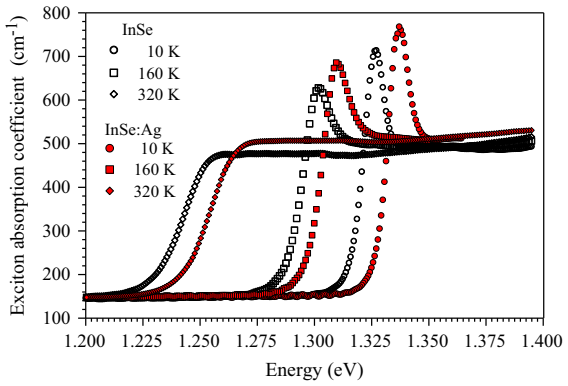

Fig. 5. Absorption spectra of InSe and InSe:Ag crystals obtained at 10, 160, and 320 K.

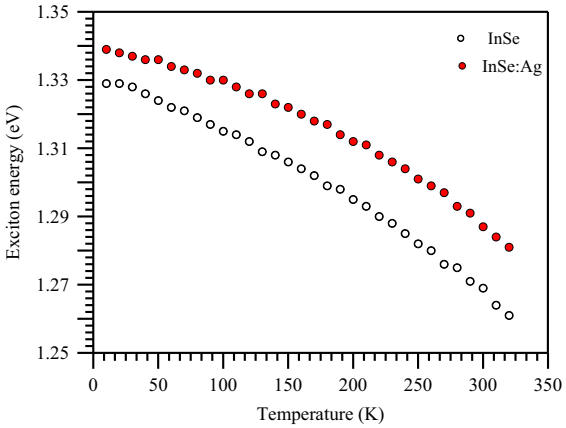

Fig. 6. The temperature dependence of the exciton energy for InSe and InS:Ag samples between 10 and 320 K temperature ranges.

Table 3
The direct band gaps and first level of exciton energy of InSe and InSe:Ag samples at different temperatures.

Samples	Sample temp. (K)	Exciton energy (eV)	Band gap energy (eV)
InSe	10	1.328 ± 0.002	1.348 ± 0.002
	160	1.304 ± 0.002	1.324 ± 0.002
	320	1.260 ± 0.002	1.280 ± 0.002
InSe:Ag	10	1.340 ± 0.002	1.360 ± 0.002
	160	1.320 ± 0.002	1.340 ± 0.002
	320	1.282 ± 0.002	1.302 ± 0.002

The experimental results for the temperature dependence of the exciton energy of undoped and Ag doped InSe in the temperature range of 10–320 K have been given in Fig. 6 dE_g/dT depends sensitively upon the terms contributing positively and negatively. It depends both on lattice expansion and electron–phonon interaction as well. The sign of temperature coefficient given in Eq. (8) neither solely depends on the sign of first term nor that of second term. The total temperature coefficient depends upon the nature of the system and especially on the electronic wave functions. There are similar examples in the IV–VI compounds and this variation depends on the specific properties of the band electronic states [17]. The temperature coefficients of exciton energies of InSe and InSe:Ag were found to have negative signs which suggests that the electron–phonon interaction term is larger than the lattice expansion contribution [3,38]. For InSe and InSe:Ag single crystals, the exciton energy values decrease towards to the lower values as the temperature increases, and the temperature coefficient has a negative sign. Such a shift is generally typical for crystals having layered structure [2,4,19,39-47].

increasing temperature. The direct band gaps were obtained by adding binding energies onto the exciton energies. The binding energies of InSe and InSe:Ag were calculated as 20.2 and 20.1 meV, respectively. The direct band gap energy for InSe and InSe:Ag samples are given in Table 3. The band gap energies and the first exciton energies in InSe:Ag are greater than those of InSe.

It is evident that the energy gap decreases with increasing temperature. The temperature coefficients δ were calculated as $4.54 \times 10^{-4} \pm 0.2$ eV/K for InSe and $3.65 \times 10^{-4} \pm 0.2$ eV/K for InSe:Ag from a satisfactory fitting of the experimental curve using the above Eq. (8). However, β for both InSe and InSe:Ag samples were calculated as 339 ± 4. As a result, Ag doping (0.01%) has caused a shift to shorter wavelength and an increase in intensity of absorption spectra. The exciton energy has increased with Ag doping.

5. Conclusions

In this research, InSe and InSe:Ag single crystals have been grown by using the Bridgman/Stockbarger method. The ingots have no cracks and voids on the surface in ingots. There is no process to polish and clean treatments at cleavage faces of these samples because of the natural mirror-like cleavage faces. InSe has specific impurities arising from its crystal structure. When transition element is doped into InSe single crystals, these impurities are eliminated by the transition elements from the crystal structure during the growth process.

We have reported the characterization of the InSe and InSe:Ag compound semiconductors by the SEM, XRD, EDX and optical absorption. It is found that the InSe and InSe:Ag crystals have

hexagonal structure. Ag doping causes a significant increase in the XRD peak intensity. The calculated lattice constants are found to be $a=4.002$ Å and $c=17.160$ Å for InSe and $a=4.619$ Å and $c=17.003$ Å for InSe:Ag. The residual strain (6.29×10^{-4} and 4.71×10^{-4} $\mathrm{lin}^{-2}/\mathrm{m}^4$) and dislocation ($4.1\times10^{14}$ and 2.0×10^{14} $\mathrm{lin}/\mathrm{m}^2$) density values have been calculated using XRD results (0 0 4), respectively. The crystallite sizes have been calculated to be 40–150 nm for InSe and 75–120 nm for InSe:Ag from the SEM results. These results are in a good agreement with EDX results. It has been observed that InSe contains In=57.12%, Se=38.08% and O=4.81%, respectively.

The optical absorption measurements of semiconductor crystals InSe and InSe:Ag have been performed as a function of temperature with 10 K increments in the range 10–320 K. The peak which gives the excitonic absorption coefficient in InSe:Ag is greater than that of InSe (Fig. 5). These are expected results, because of the behaviour of the Ag atoms in the InSe. The Ag doping causes a new appearance in terms of the band gap energy and increases in the intensity of excitonic absorption peak in InSe. The increase in the slope is due to the disappearance of impurities in the undoped materials by Ag doping. This result shows that there are many impurities in InSe single crystal and these impurities in InSe are compensated by Ag doping.

Acknowledgements

This work was supported by the Atatürk University Research Fund, Project no: 2012/458, 2012/461, 2013/286, 2013/311.

References

[1] E. Mooser, in: (Ed.), Physics and Chemistry of Material With Layered Structure, Riedel:Dordrecht, 1976.
[2] Z.D. Kovalyuk, V.M. Katerynchuk, I.V. Mintyanskii, A.I. Savchuk, O.M. Sydor, Mater. Sci. Eng., B 118 (2005) 147.
[3] B.G. Tagiev, G.M. Niftiev, F.Sn. Aidaev, Phys. Status Solidi A 89 (1985) 639.
[4] B. Gürbulak, M. Kundakçı, A. Ateş, M. Yıldırım, Phys. Scr. 75 (2007) 424.
[5] S.M. El-Sayed, Vacuum 72 (2003) 169.
[6] J.Y. Emery, L. Brahimotsmane, M. Jouanne, C. Julien, M. Balkanski, Mater. Sci. Eng., B 3 (1989) 13.
[7] C. Julien, N. Benramdane, J.P. Guesdon, Semicond. Sci. Technol. 5 (1990) 905.
[8] Jin-Ho Park, M.A. Fzaal, M. Helliwell, M.A. Malik, P. O'Brien, J. Raftery, Chem. Mater. 15 (2003) 4205.
[9] O. Lang, A. Klein, C. Pettenkofer, W. Jaegermann, J. Appl. Phys. 80 (1996) 3817.
[10] O.A. Balitskii, R.V. Lutsiv, V.P. Savchyn, J.M. Stakhira, Mater. Sci. Eng., B 56 (1998) 5.
[11] B. Kobbi, D. Ouadjaout, N. Kesri, Vacuum 62 (2001) 321.
[12] T. Siciliano, A. Tepore, G. Micocci, A. Genga, M. Siciliano, E. Filippo, J. Mater. Sci. - Mater. Electron. 22 (2011) 649.
[13] D.Y. Lyu, T.Y Lin, T.W Chang, S.M. Lan, T.N. Yang, C.C Chiang, C.L. Chen, H.P. Chiang, J. Alloys Compd. 499 (2010) 104.
[14] A. Hirohata, J.S. Moodera, G.P. Berera, Thin Solid Films 510 (2006) 247.
[15] L. Sidong, G. Liehui, N. Sina, A. George, R. Kappera, J. Lou, M. Chhowalla, H. Yamaguchi, G. Gupta, R. Vajtai, A.D. Mohite, P.M. Ajayan, ACS Nano 8 (2) (2014) 1263.
[16] A.B. Abd El- Moiz, Physica B 191 (1993) 293.
[17] B. Gürbulak, Solid State Commun. 109 (1999) 665.
[18] A. Ateş, B. Gürbulak, M. Yıldırım, S. Doğan, Physica E 16 (2003) 274.
[19] W. Mudd Garry, A. Svatek Simon, T. Ren, A.P. Amolia, M. Oleg, E. Laurence, B.H. Peter, K.K. Zakhar, L.V. Kovalyuk, K.R. Zakhar, D.I. Alexandr, Adv. Mater. 25 (40) (2013) 5714.
[20] K. Imai, K. Suzuki, T. Haga, Y. Hasegawa, Y. Abe, J. Cryst. Growth 54 (1981) 501.
[21] B.D. Cullity, Elements of X-ray Diffraction, Addison Wesley, Reading, MA (1972) 102.
[22] M.M. Abdullah, G. Bhagavannarayana, M.A. Wahab, J. Cryst. Growth 312 (2010) 1534.
[23] Y.P. Varshni, Physica 34 (1967) 149.
[24] H.J. Gysling, A.A. Wernberg, T.N. Blanton, Chem. Mater. 4 (1992) 900.
[25] I.-H. Choi, P.Y. Yu, J. Appl. Phys. 93 (2003) 4673.
[26] C. Viswanathan, S. Gopal, M. Thamilselvan, K. Premnazeer, D. Mangalaraj, S.K. Narayandass, J. Yi, D.C. Ingram, J. Mater. Sci. - Mater. Electron. 15 (2004) 787.
[27] C. Viswanathan, V. Senthilkumar, R. Sriranjini, D. Mangalaraj, S.K. Narayandass, J. Yi, Cryst. Res. Technol. 40 (2005) 658.
[28] A. Hirohata, J.S. Moodera, G.P. Berera, Thin Solid Films 510 (2006) 247.
[29] A. Ateş, M. Kundakçı, A. Astam, M. Yıldırım, Physica E 40 (2008) 2709.
[30] T. Siciliano, A. Tepore, G. Micocci, A. Genga, M. Siciliano, E. Filippo, J Mater Sci: Mater. Electron. 22 (2011) 649.
[31] D.H. Mosca, N. Mattoso, C.M. Lepienski, W. Veiga, I. Mazzaro, V.H. Etgens, M. Eddrief, J. Appl. Phys. 91 (2002) 140.
[32] H.K Park, K. Jang, S. Kim, J.H. Kim, S.S. Uk, J. Am. Chem. Soc. 128 (2006) 14780.
[33] O.A. Balitskii, R.V. Lutsiv, V.P. Savchyn, J.M. Stakhira, Materials Science and Engineering B 56 (1998) 5.
[34] B. Gürbulak, M. Yildirim, A. Ateş, S. Dogan S, Y.K. Yoğurtçu, Jpn. J. Appl. Phys. 38 (1999) 5133.
[35] M. Zolfaghari, K.P. Jain, H.S. Mavi, M. Balkanski, C. Julien, A. Chevy, Mater. Sci. Eng. B 38 (1996) 161.
[36] K. Ravichandran, B. Sakthivel, P. Philominathan, Cryst. Res. Technol. 45 (2010) 292.
[37] S. Doğan, S. Tüzemen, B. Gürbulak, A. Ateş, M. Yıldırım, J. Appl. Phys. 85 (9) (1999) 6777.
[38] V.A. Aliev, E.F. Bagirzade, N.Z. Gasanov, G.D. Guseinov, Sov. Phys. Solid State 29 (1987) 1.
[39] Y.P. Gnatenko, Z.D. Kovalyuk, P.A. Skubesko, Phys. Status Solidi B 106 (1981) 621.
[40] C. De Blasi, G. Micocci, S. Mongelli, A. Tepore, J. Cryst. Growth. 57 (1982) 482.
[41] V. Riede, H. Neumann, F. Levy, H. Sobotta, Phys. Status Solidi B 109 (1982) 275.
[42] R. Tenne, B. Thets, J. Rioux, C. Levy-Clement, J. Appl. Phys. 57 (1985) 141.
[43] M. Kundakçı, B. Gürbulak, S. Doğan, A. Ateş, M. Yıldırım, Appl. Phys. A Mater. Sci. Process. 90 (2008) 479.
[44] B. Gürbulak, Phys. Scr. 70 (2004) 197.
[45] B. Gürbulak, Physica Scripta 70 (2004) 197.
[46] S. Gopal, C. Viswanathan, B. Karunagaran, Sa. K. Narayandass, D. Mangalaraj, Junsin Yi, Cryst. Res. Technol. 40 (No. 6) (2005) 557.
[47] A.A.A. Darwish, M.M. El-Nahass, M.H Bahlol, Appl. Surf. Sci. 276 (2013) 210.